

f-Band Ferromagnetism in the Periodic Anderson Model – a Modified Alloy Analogy

G G Reddy[†], D Meyer[‡], S Schwieger[‡], A Ramakanth[†] and W Nolting[‡]

[†]Department of Physics, Kakatiya University, Warangal-506009, India

[‡]Institut für Physik, Humboldt-Universität zu Berlin, D-10115 Berlin, Germany

Abstract. We introduce a new approximation scheme for the periodic Anderson model (PAM). The modified alloy approximation represents an optimum alloy approximation for the strong coupling limit, which can be solved within the CPA-formalism. Zero-temperature and finite-temperature phase diagrams are presented for the PAM in the intermediate-valence regime. The diversity of magnetic properties accessible by variation of the system parameters can be studied by means of quasiparticle densities of states: The conduction band couples either ferro- or antiferromagnetically to the *f*-levels. A finite hybridization is a necessary precondition for ferromagnetism. However, too strong hybridization generally suppresses ferromagnetism, but can for certain system parameters also lead to a semi-metallic state with unusual magnetic properties. By comparing with the spectral density approximation, the influence of quasiparticle damping can be examined.

PACS numbers: 75.30.Mb 71.28.+d 71.10.Fd 75.20.Hr

1. Introduction

Correlated electron systems have come to occupy the centre stage in both theory and experiment in condensed matter physics. There is a general consensus that strong electron correlations play a decisive role in a variety of phenomena such as magnetism, heavy fermions, high-temperature superconductivity, colossal magneto-resistance etc. The real systems that display these phenomena are transition metals (3d), alloys and compounds as well as rare earth (4f) systems (metals, insulators), in particular cuprates, manganites, Ce compounds etc.. There is intense activity both theoretically and experimentally to isolate the essential interactions responsible for these phenomena. In this process, several model systems are being studied which are expected to at least qualitatively mimic the actual systems in some region or the other of the parameter space. One of the most widely used models which brings out the role of electron correlations while also taking into account the interplay of two different types of electrons, one highly localized and the other quasi free, is the well-known Anderson model [1]. One distinguishes the "single impurity Anderson model" (SIAM), if the system of uncorrelated conduction electrons hybridizes with a single localized state, and

the "periodic Anderson model" (PAM), if the hybridization takes place with a periodic lattice of localized states. As far as the SIAM is concerned many exact results have been obtained, e. g. by using Bethe ansatz [2] or renormalization group theory [3]. Very recently the SIAM has gained a new upsurge in connection with the "dynamical mean field theory" [4, 5, 6] that exploits the fact that in infinite lattice dimensions theoretical lattice models like the Hubbard model can be mapped onto single-impurity models such as the SIAM. Numerically essentially exact methods such as the exact diagonalization of small systems, quantum Monte Carlo calculations or numerical renormalization group theory [6, 7] have provided further insight into the physics of the model. However, since these numerical methods are bound to certain limitations, reliable analytical approaches remain to be required [8].

The situation is less satisfactory in the case of the PAM. Even though there exists a number of approximate schemes for different parameter constellations, referring to either of the so-called heavy fermion, intermediate valence and Kondo regimes, there is still need for further improvement and extension. The matter acquires additional urgency in view of the fact that for the parameter space corresponding to strongly correlated low-lying localized states the PAM can be mapped [9] on to the Kondo lattice model [10] which is of great current interest, e. g. with respect to the extraordinary physical properties of the manganites [11].

Recently we proposed a new approximation scheme [12] which is based on a mapping of the PAM on to an effective Hubbard model. The parameters of the Hubbard model are such that they correspond to the strong coupling limit. Therefore we could exploit a reliable approximate theory, trustworthy in the strong coupling limit. Such a theory is the "spectral density approach" (SDA) [13, 14, 15]. Its main advantages are the physically simple concept and the non-perturbative character. In this scheme we have studied the magnetic $T = 0$ -phase diagram of the PAM as well as its finite temperature magnetic properties. The SDA, however, shows up a principal limitation concerning quasiparticle damping. By ansatz the SDA self-energy is a real quantity, thus neglecting from the very beginning effects due to finite lifetimes of the quasiparticles. How quasiparticle damping influences the magnetic stability in the PAM is an interesting and important question having been left open by our previous theory [12]. It is the main impetus for the present study to close this gap.

A conceptionally simple method that is able to provide complex self-energies is the "coherent potential approximation" (CPA) [16]. In order to perform CPA on the PAM, we have to fix up an alloy analogy. This requires the determination of the energy levels and the concentrations of the components of the fictitious alloy. Within the conventional alloy analogy treatment (AA) due to Hubbard [17] these are taken by referring to the atomic limit. For an application to the PAM, see e. g. [18, 19]. However, this choice is by no means predetermined. On the contrary it can be shown that it is indeed not the best ansatz. One knows that CPA becomes an exact procedure in infinite lattice dimensions ($d = \infty$), where the inherent single-site aspect of CPA is rigorous [20]. However, the CPA-solution of the AA for the $d = \infty$ -Hubbard model violates the exactly known

strong coupling behaviour [21] and also does not reproduce the weak coupling results of second order perturbation theory [22, 23]. Furthermore it contradicts exact high-energy expansions [24]. So we have to conclude that the conventional AA, which starts from the atomic limit solution, is not the most convenient alloy analogy. In this paper we therefore derive the "modified alloy analogy" (MAA), which was recently introduced for the Hubbard model[25, 24], for the PAM. This method substantially improves the AA ansatz by deriving the proper alloy analogy from exact high energy expansions of the single-electron Green function and the self-energy, respectively. This procedure guarantees the correct strong coupling behaviour relevant for the PAM. On the way of deriving the MAA, the above-mentioned SDA can easily be re-derived without the necessity of introducing the effective Hubbard model as was done before[12]. It turns out that the "atomic levels" of fictitious alloy constituents are nothing else but the SDA-quasiparticle energies in the zero-bandwidth limit. Similarly the "concentrations" agree with the SDA-spectral weights in this limit. The MAA therewith promises to keep the advantages of the SDA while simultaneously improving the method by incorporating quasiparticle damping. The SDA-energies and spectral weights contain non-trivial thermodynamic expectation values which have to be determined self-consistently. By them the itineracy of the $-\sigma$ -electrons, which define the fictitious alloy for the propagating σ -electrons, comes into play, at least to a certain degree. The neglect of this itineracy is a well-known shortcoming of the conventional AA.

The paper is organized as follows. In the next section the PAM and its many-body problem is formulated. An approximate solution by use of the MAA scheme is then developed in section 3. Section 4 is devoted to a presentation and discussion of the results concerning the magnetic properties of the PAM. The paper ends with some concluding remarks.

2. Model Hamiltonian and Its Many-Body Problem

Starting point is the periodic Anderson Hamiltonian

$$H = \sum_{ij\sigma} (T_{ij} - \mu) s_{i\sigma}^\dagger s_{j\sigma} + \sum_{i,\sigma} (e_f - \mu) f_{i\sigma}^\dagger f_{i\sigma} + \quad (1)$$

$$+ V \sum_{i,\sigma} (f_{i\sigma}^\dagger s_{i\sigma} + s_{i\sigma}^\dagger f_{i\sigma}) + \frac{1}{2} U \sum_{i,\sigma} n_{i\sigma}^{(f)} n_{i-\sigma}^{(f)} \quad (2)$$

$s_{i\sigma}$ ($f_{i\sigma}$) and $s_{i\sigma}^\dagger$ ($f_{i\sigma}^\dagger$) are, respectively, the annihilation and the creation operators for an electron in a non-degenerate conduction band (localized f -state), and $n_{i\sigma}^{(f)} = f_{i\sigma}^\dagger f_{i\sigma}$ is the spin-dependent occupation number operator for the f -state. The index i refers to the respective lattice site, $\sigma = \{\uparrow, \downarrow\}$ is the spin projection. The hopping integral T_{ij} ,

$$T_{ij} = \frac{1}{N} \sum_{\mathbf{k}} e^{-i\mathbf{k}\cdot(\mathbf{R}_i - \mathbf{R}_j)} \epsilon(\mathbf{k}) \quad (3)$$

describes the propagation of a band electron from site R_j to site R_i . $\epsilon(\mathbf{k})$ is the free Bloch energy, while e_f denotes the position of the non-degenerate f -level. We choose

the energy zero to coincide with the centre of gravity of the unperturbed conduction band:

$$T_{ii} = \frac{1}{N} \sum_{\mathbf{k}} \epsilon(\mathbf{k}) \stackrel{!}{=} 0 \quad (4)$$

U is the intra-atomic Coulomb repulsion between f -electrons. The hybridization V is taken as a real and \mathbf{k} -independent local matrix element, μ is the chemical potential.

Let us start with the retarded single- $s(f)$ electron Zubarev Green's function

$$G_{ij\sigma}^{(f)}(E) = \langle\langle f_{i\sigma}; f_{j\sigma}^\dagger \rangle\rangle; \quad G_{ij\sigma}^{(s)}(E) = \langle\langle s_{i\sigma}; s_{j\sigma}^\dagger \rangle\rangle \quad (5)$$

$$G_{\mathbf{k}\sigma}^{(f,s)} = \frac{1}{N} \sum_{\mathbf{k}} e^{i\mathbf{k}\cdot(\mathbf{R}_i - \mathbf{R}_j)} G_{ij\sigma}^{(f,s)}(E) \quad (6)$$

The equations of motion are easily derived and formally solved,

$$G_{\mathbf{k}\sigma}^{(s)}(E) = \hbar \frac{E - (e_f - \mu) - \Sigma_{\mathbf{k}\sigma}(E)}{(E - (e_f - \mu) - \Sigma_{\mathbf{k}\sigma}(E))(E - (\epsilon(\mathbf{k}) - \mu)) - V^2} \quad (7)$$

$$G_{\mathbf{k}\sigma}^{(f)}(E) = \frac{\hbar}{E - (e_f - \mu) - \frac{V^2}{E - (\epsilon(\mathbf{k}) - \mu)} - \Sigma_{\mathbf{k}\sigma}(E)} \quad (8)$$

where the self-energy $\Sigma_{\mathbf{k}\sigma}(E)$ has been introduced via

$$\Sigma_{\mathbf{k}\sigma}(E) G_{\mathbf{k}\sigma}^{(f)}(E) = U \frac{1}{N} \sum_{\mathbf{p}, \mathbf{q}} \langle\langle f_{\mathbf{p}\sigma}^\dagger f_{\mathbf{q}-\sigma} f_{\mathbf{p}+\mathbf{k}-\mathbf{q}\sigma}; f_{\mathbf{k}\sigma}^\dagger \rangle\rangle \quad (9)$$

Obviously the explicitly problem is solved as soon as we have found a solution for the self-energy. The f - and s -quasiparticle densities of states (QDOS) are given by

$$\rho_{\sigma}^{(s)}(E) = -\frac{1}{\pi\hbar N} \sum_{\mathbf{k}} \Im G_{\mathbf{k}\sigma}^{(s)}(E - \mu + i0^+) \quad (10)$$

$$\rho_{\sigma}^{(f)}(E) = -\frac{1}{\pi\hbar N} \sum_{\mathbf{k}} \Im G_{\mathbf{k}\sigma}^{(f)}(E - \mu + i0^+) \quad (11)$$

and determine the spin-dependent average occupation number $n_{\sigma}^{(s,f)}$, which we need to construct the magnetic phase diagram of the PAM:

$$n_{\sigma}^{(s)} = \langle s_{i\sigma}^\dagger s_{i\sigma} \rangle = \int_{-\infty}^{+\infty} dE f_{-}(E) \rho_{\sigma}^{(s)}(E) \quad (12)$$

$$n_{\sigma}^{(f)} = \langle f_{i\sigma}^\dagger f_{i\sigma} \rangle = \int_{-\infty}^{+\infty} dE f_{-}(E) \rho_{\sigma}^{(f)}(E) \quad (13)$$

3. Modified alloy analogy

A standard method to solve many-body problems as that posed by the PAM Hamiltonian (1) is the CPA [16]. As a single-site approximation the resulting f -electron self-energy will be local, i. e. \mathbf{k} -independent. If we apply this method here we have to solve the following equation self-consistently

$$0 = \sum_{p=1}^n x_{p\sigma} \frac{E_{p\sigma} - \Sigma_{\sigma}(E) - e_f}{1 - \frac{1}{\hbar} G_{ii\sigma}^{(f)}(E)(E - \Sigma_{\sigma}(E) - e_f)} \quad (14)$$

$$G_{ii\sigma}^{(f)}(E) = \frac{1}{N} \sum_{\mathbf{k}} G_{\mathbf{k}\sigma}^{(f)}(E); \quad \Sigma_{\sigma}(E) = \frac{1}{N} \sum_{\mathbf{k}} \Sigma_{\mathbf{k}\sigma}(E) \quad (15)$$

The solution of (14) needs to fix the alloy analogy, i. e. the "atomic levels" $E_{p\sigma}$ and the "concentrations" $x_{p\sigma}$ of the n constituents of the fictitious alloy. Since the dominant features of the correlated f -level in the PAM are the two charge excitations separated by U , the number of "alloyed" components n is set to two. The conventional alloy analogy (AA) uses the $V = 0$ limit ("atomic" limit) of the PAM to determine $E_{p\sigma}$ and $x_{p\sigma}$ [18, 19]:

$$\begin{aligned} E_{1\sigma}^{(AA)} &= e_f; & x_{1\sigma}^{(AA)} &= n_{-\sigma}^{(f)} \\ E_{2\sigma}^{(AA)} &= e_f + U; & x_{2\sigma}^{(AA)} &= 1 - n_{-\sigma}^{(f)} \end{aligned} \quad (16)$$

The result violates the weak as well as the strong coupling behaviour and as for the Hubbard model prohibits spontaneous magnetism [18, 26, 27, 24]. In particular the strong coupling behaviour appears to be crucial with respect to ferromagnetism. On the other hand, the choice (16) is not at all predetermined. We propose another way to find out the "best alloy analogy". Correct strong coupling behaviour is guaranteed by fulfilling the high-energy expansion of relevant Green functions and self-energies [24]. Decisive ingredients for proper high-energy expansions are the local spectral moments

$$\begin{aligned} M_{\sigma}^{(n)} &= \frac{1}{N} \sum_{\mathbf{k}} M_{\mathbf{k}\sigma}^{(n)}; \quad n = 0, 1, 2, \dots \\ M_{\mathbf{k}\sigma}^{(n)} &= \frac{1}{\hbar} \int dE E^n S_{\mathbf{k}\sigma}(E) \end{aligned} \quad (17)$$

$S_{\mathbf{k}\sigma}(E)$ is the f -electron spectral density:

$$S_{\mathbf{k}\sigma}(E) = -\frac{1}{\pi} \Im G_{\mathbf{k}\sigma}^{(f)}(E + i0^+) \quad (18)$$

The moments can be calculated independently of the required spectral density:

$$M_{\mathbf{k}\sigma}^{(n)} = \langle \underbrace{[[\dots [f_{\mathbf{k}\sigma}, H]_-, \dots, H]_-}_{n\text{-fold commutator}}, f_{\mathbf{k}\sigma}^{\dagger}]_+ \rangle \quad (19)$$

$[\dots, \dots]_-$ denotes the commutator and $[\dots, \dots]_+$ the anti-commutator. For the Green function (5) we can write

$$G_{\mathbf{k}\sigma}^{(f)}(E) = \int dE' \frac{S_{\mathbf{k}\sigma}(E')}{E - E'} = \hbar \sum_{n=0}^{\infty} \frac{M_{\mathbf{k}\sigma}^{(n)}}{E^{n+1}} \quad (20)$$

For solving the CPA-equation (14) we only need the local spectral moments which are found to be

$$\begin{aligned} M_{\sigma}^{(0)} &= 1 \\ M_{\sigma}^{(1)} &= e_f + Un_{-\sigma}^{(f)} \\ M_{\sigma}^{(2)} &= e_f^2 + 2e_f Un_{-\sigma}^{(f)} + U^2 n_{-\sigma}^{(f)} + V^2 \\ M_{\sigma}^{(3)} &= e_f^3 + 3e_f^2 Un_{-\sigma}^{(f)} + U^2 e_f (2n_{-\sigma}^{(f)} + n_{-\sigma}^{(f)2}) + U^3 n_{-\sigma}^{(f)} + \\ &+ V^2 (2e_f + 2Un_{-\sigma}^{(f)} + T_{ii}) + U^2 n_{-\sigma}^{(f)} (1 - n_{-\sigma}^{(f)}) B_{-\sigma} \end{aligned} \quad (21)$$

From (8) we get the corresponding expansion for the self-energy:

$$\Sigma_{\mathbf{k}\sigma}(E) = \sum_{n=0}^{\infty} \frac{C_{\mathbf{k}\sigma}^{(n)}}{E^n}; \quad \Sigma_{\sigma}(E) = \frac{1}{N} \sum_{\mathbf{k}} \Sigma_{\mathbf{k}\sigma}(E) \quad (22)$$

with the local coefficients:

$$\begin{aligned} C_{\sigma}^{(0)} &= Un_{-\sigma}^{(f)} \\ C_{\sigma}^{(1)} &= U^2 n_{-\sigma}^{(f)} (1 - n_{-\sigma}^{(f)}) \\ C_{\sigma}^{(2)} &= U^2 n_{-\sigma}^{(f)} (1 - n_{-\sigma}^{(f)}) (B_{-\sigma} + U(1 - n_{-\sigma}^{(f)})) \end{aligned} \quad (23)$$

Surprisingly the hybridization V does not explicitly appear in the $C_{\sigma}^{(n)}$. The contributions via the moments (21) are exactly cancelled by those from the term $\frac{V^2}{E - (\epsilon(\mathbf{k}) - \mu)}$ in (8).

By use of (20) and (22) we now expand the CPA-equation (14) with respect to powers of $\frac{1}{E}$. Comparison of the coefficients of the $\frac{1}{E^n}$ terms up to $n = 3$ yields the following set of four equations for the four unknown quantities $E_{(1,2)\sigma}$ and $x_{(1,2)\sigma}$:

$$\begin{aligned} \sum_{p=1}^2 x_{p\sigma} &= 1 \\ \sum_{p=1}^2 x_{p\sigma} (E_{p\sigma} - e_f) &= Un_{-\sigma}^{(f)} \\ \sum_{p=1}^2 x_{p\sigma} (E_{p\sigma} - e_f)^2 &= U^2 n_{-\sigma}^{(f)} \\ \sum_{p=1}^2 x_{p\sigma} (E_{p\sigma} - e_f)^3 &= U^3 n_{-\sigma}^{(f)} + U^2 n_{-\sigma}^{(f)} (1 - n_{-\sigma}^{(f)}) (B_{-\sigma} - e_f) \end{aligned} \quad (24)$$

We now use eqs. (24) to fix the "optimum" alloy analogy. After simple manipulations we get

$$\begin{aligned} E_{1,2\sigma} &= \frac{1}{2} [B_{-\sigma} + U + e_f \pm \sqrt{(B_{-\sigma} + U - e_f)^2 + 4Un_{-\sigma}^{(f)}(e_f - B_{-\sigma})}] \\ x_{1\sigma} &= \frac{E_{2\sigma} - e_f - Un_{-\sigma}^{(f)}}{E_{2\sigma} - E_{1\sigma}} = 1 - x_{2\sigma} \end{aligned} \quad (25)$$

The decisive point for the ongoing procedure is the "higher" correlation function $B_{-\sigma}$:

$$n_{-\sigma}^{(f)} (1 - n_{-\sigma}^{(f)}) (B_{-\sigma} - e_f) = V \langle f_{i-\sigma}^{(\dagger)} s_{i-\sigma} (2n_{i\sigma}^{(f)} - 1) \rangle \quad (26)$$

It has been elaborated in previous works [13, 14, 15, 24] that its analogue has a decisive influence on the stability at spontaneous magnetism in the Hubbard model. We believe, it plays a similarly important role for ferromagnetism in the PAM[12, 28]. In spite of the fact that it is a "higher" correlation function it can rigorously be expressed by single-electron terms [13]:

$$n_{-\sigma}^{(f)} (1 - n_{-\sigma}^{(f)}) (B_{-\sigma} - e_f) = -\frac{1}{\pi\hbar} \Im \int_{-\infty}^{+\infty} dE f_{-}(E) \left(\frac{2}{U} \Sigma_{\sigma}(E) - 1 \right) \quad (27)$$

$$\times \left((E - (e_f - \mu) - \Sigma_\sigma(E)) G_{ii\sigma}^{(f)}(E) - \hbar \right)$$

With the fictitious alloy (25), we enter the CPA-equation (14). The theory is now complete. The equations (14), (15), (8), (27) and (13), together with (25) build a closed system of equations which can be solved self-consistently for the self-energy $\Sigma_\sigma(E)$. Note that the only \mathbf{k} -dependence comes into play by (8) via the formal solution of the equation of motion. The \mathbf{k} -dependence is therefore strictly an $\epsilon(\mathbf{k})$ -dependence, so that all \mathbf{k} -summations can be replaced by simpler energy-integration over the "free" Bloch density of states $\rho_0(E) = 1/N \sum_{\mathbf{k}} \delta(E - \epsilon(\mathbf{k}))$ which has to be considered as a model parameter:

$$G_{ii\sigma}^{(f)}(E) = \hbar \int_{-\infty}^{+\infty} dx \frac{\rho_0(x)}{E - (e_f - \mu) - \frac{V^2}{E - (x - \mu)} - \Sigma_\sigma(E)} \quad (28)$$

Let us comment on the modified alloy analogy (25) and its differences to the conventional AA (16): Within the AA, the σ -*f* electron is propagating through a fictitious alloy where one component is represented by lattice sites with no $-\sigma$ -electron present, and the other component by lattice sites which are occupied by one $-\sigma$ electron. This approach therefore completely neglects the hybridization between the *f*-levels and the conduction band. For calculating the self-energy, the $-\sigma$ *f*-electrons are frozen, any exchange with the conduction band is eliminated. This excludes the possibility of magnetic order in the system. How can this drawback be circumvented? It is clear that the PAM will always be considered to belong to the strong coupling regime (large U). Two well separated excitation peaks will therefore be expected in the *f*-electron quasiparticle density of states. The above-described ansatz of fitting the positions and weights of these to an exact $\frac{1}{E}$ -expansion of the Green function seems the most plausible one since these charge excitation peaks themselves are high-energy features. It is noteworthy that all thereby induced differences between the MAA and the AA are due to the hybridization between *f*- and *s*-levels. It can be seen in equation (26) that in the limit of vanishing hybridization ($V = 0$), $B_{-\sigma} = e_f$ holds and equations (25) reduce to the conventional alloy analogy (16). However, for finite hybridization, $B_{-\sigma}$ and $n_{-\sigma}^{(f)}$ are to be determined self-consistently by (27) and (13), respectively, possibly providing the alloy energies and concentrations with an explicit spin-dependence. In each step of the CPA-iteration $B_{-\sigma}$ and $n_{-\sigma}^{(f)}$ may change and so does the underlying fictitious alloy. Equation (26) makes clear that the inclusion of $B_{-\sigma}$ accounts to a certain degree for the hybridization of $-\sigma$ -*f*-electrons with the conduction band and therefore also to their effective itineracy which is completely neglected in the conventional alloy analogy (16).

Before further discussing the MAA, let us remind the reader of the already mentioned spectral density approximation (SDA). In a previous work, this theory was derived via mapping of the PAM onto an effective medium Hubbard model [12]. Within this effective Hubbard model, the SDA is justified in the strong coupling limit where the obtained positions and spectral weights of the lower and upper Hubbard band coincide with exact results up to the order $\frac{1}{U}$ [21]. At this point it is noteworthy that exactly the

same results as in reference[12] can also be obtained by adapting the concept of the SDA directly onto the PAM which is possible and straightforward from the above-presented results. Motivated by the solution of the “atomic” limit ($V = 0$) we make the following ansatz for the self-energy:

$$\Sigma_\sigma(E) = \alpha_{1\sigma} \frac{E - \alpha_{2\sigma}}{E - \alpha_{3\sigma}} \quad (29)$$

The coefficients of this ansatz can now be fitted in such a way that the high energy expansion of the self-energy, (22) with the coefficients (23) is fulfilled. One readily arrives at

$$\Sigma_\sigma^{(\text{SDA})}(E) = \frac{U n_{-\sigma}^{(f)} (E - B_{-\sigma} - e_f)}{E - B_{-\sigma} - e_f - U(1 - n_{-\sigma}^{(f)})} \quad (30)$$

which together with equations (28), (27) and (13) solves the problem. It is straightforward to show that this is identical to the approximation proposed in reference [12]. Therefore, the discussion of the advantages and disadvantages of the method found therein remains valid. The main disadvantage was clearly the neglection of quasiparticle damping in the ansatz (29).

Now turning back to the MAA, its benefits are immediately clear. While reproducing the high-energy expansion up to the same order as the SDA, it additionally incorporates quasiparticle damping via the CPA formalism. And contrary to the conventional alloy analogy, the freedom of defining the “alloyed components” is used to ensure the correct high-energy expansion (22).

We conclude that the essentials of the qualitatively convincing SDA used in our previous paper [12] are incorporated in the MAA and completed by a proper quasiparticle damping. So the MAA represents a systematic improvement and extension of the SDA. Comparison of results for MAA and SDA will allow to inspect very directly the influence of quasiparticle damping on magnetic stability in the PAM.

4. Results and Discussion

The presented theory for the periodic Anderson model has been evaluated for a system characterized by the following parameters: The free conduction band density of states is chosen to be semi-elliptic with a width of $W = 1\text{eV}$ centred at $E = 0$. The f -level is determined by its distance (e_f) to the conduction band centre and the intraatomic Coulomb interaction U . The latter is 4eV throughout the paper. That means we consider the PAM in the strong coupling regime. Furthermore, we are mainly interested in the intermediate valence regime, i. e. e_f is presumed to be located within the Bloch-band region ($-0.5\text{eV} < e_f < +0.5\text{eV}$). It turns out that the physics of the PAM strongly depends on the total particle density

$$n^{(\text{tot})} = \sum_\sigma (n_\sigma^{(f)} + n_\sigma^{(s)}); \quad 0 \leq n^{(\text{tot})} \leq 4 \quad (31)$$

We therefore present results for different $n^{(\text{tot})}$, but so that the upper charge excitation at $e_f + U$ (“upper Hubbard band”) remains in any case unoccupied ($n^{(\text{tot})} < 3$). Another

decisive variable is of course the temperature T given in Kelvin. The evaluation of our theory has been done for a translational symmetric lattice, antiferromagnetic ordering is not considered. We rather concentrate ourselves on the possibility and the conditions of spontaneous ferromagnetism.

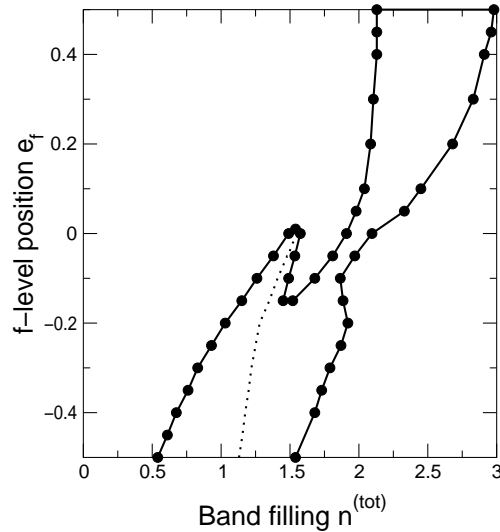


Figure 1. Magnetic phase diagram in the $n^{(\text{tot})}$ - e_f plane for $V = 0.1$, $U = 4$ and $T = 0$. f - and s -magnetizations are parallel to the left of the dotted line and anti-parallel to the right.

The magnetic phase diagram in terms of $n^{(\text{tot})}$ and e_f for a small hybridization $V = 0.1\text{eV}$ is plotted in figure 1. For a given e_f within the Bloch band region ferromagnetism becomes possible for particle densities in between a lower and an upper critical value. These critical values shift to higher numbers with increasing f -level position. Ferromagnetism is of course basically provoked by the correlated f -electrons. Except for the hybridization with the conduction electrons they are described by the zero-bandwidth Hubbard model. The latter special case, however, forbids ferromagnetism. So a finite hybridization V is needed. On the other hand, one knows that ferromagnetic spin order in the Hubbard model is bound to further conditions: The band occupation and the Coulomb correlation U/W must exceed critical values which are different for different lattice structures [14, 15, 29, 30]. Furthermore, the free band should have an assymetric density of states[31]. SDA and MAA both do not allow ferromagnetism in the "pure" Hubbard model for highly symmetric free densities of states such as the semi-elliptic one irrespective of the correlation strength U/W . In the PAM with finite hybridization V , however, all these conditions can be met: The hybridization creates a finite width of the f -dispersion, and the resulting effective f -band turns out to be strongly asymmetric, therewith allowing for a ferromagnetic ground state. For a given e_f the lower critical density in the phase diagram (figure 1) is the analogue to the critical particle density in the Hubbard model [15]. At the upper boundary the lower f -charge excitation is more or less filled corresponding to a half-filled band in the

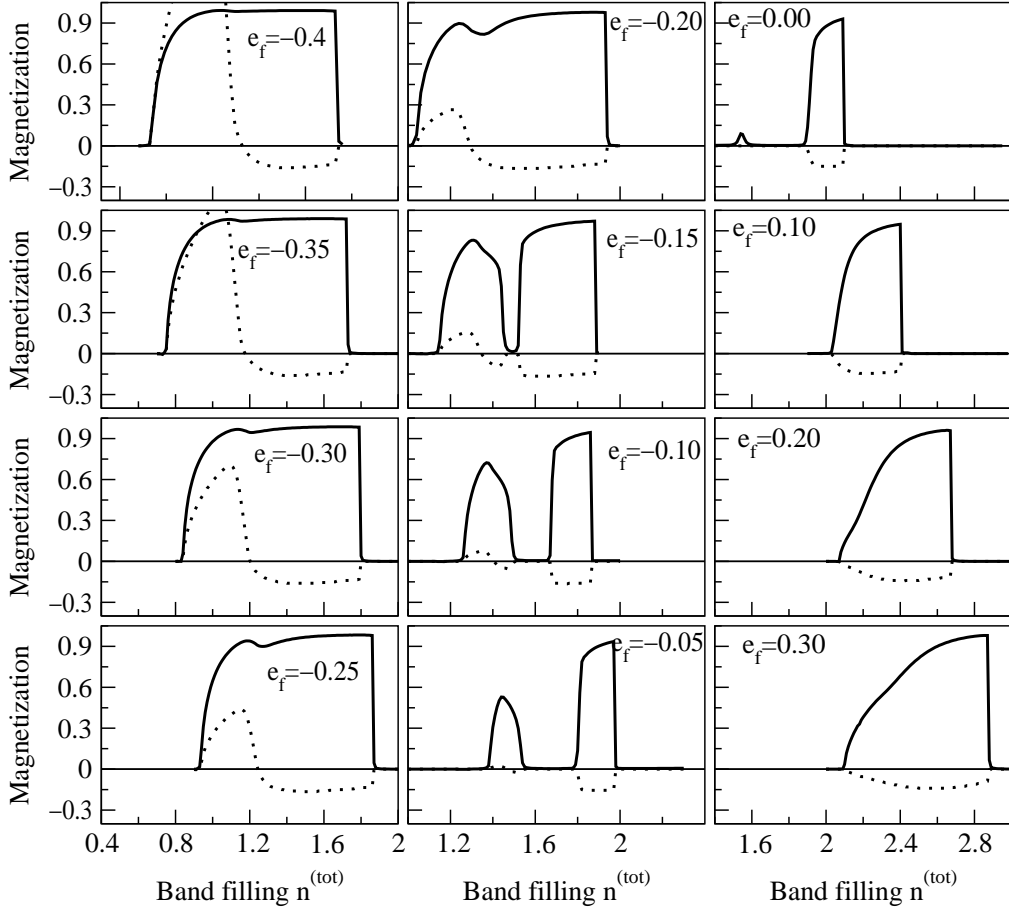


Figure 2. f - (solid line) and s - (dotted line) magnetizations as a function of $n^{(\text{tot})}$ for various values of e_f . The s -magnetization is multiplied by a factor of 5 for better visibility. Other parameters are as in figure 1.

strongly coupled Hubbard model for which antiferromagnetism is to be expected[32, 15].

The upper boundary in the phase diagram for a given e_f corresponds always to a first order transition, the lower one to a second order transition. This can be seen in figure 2 where the spontaneous $T = 0$ -magnetization is plotted as function of the total particle density $n^{(\text{tot})}$. The position of the f -level leads to strikingly different behaviour of the magnetization.

With e_f in the lower half of the conduction band (left column in figure 2) the f -magnetization increases from the lower boundary very rapidly into saturation in order to perform the mentioned discontinuous transition into the paramagnetic phase at the upper boundary. Interesting is the induced s -polarization starting positive (ferromagnetic s - f coupling) for weak electron densities and changing its sign (antiferromagnetic s - f coupling) at about $n^{(\text{tot})} = 1.2$. According to the Schrieffer-Wolff transformation [9] at first glance an antiferromagnetic coupling between s -and f -electrons would be expected. However, the transformation is bound to the Kondo-limit ($n^{(f)} = 1$) and is not necessarily conclusive for the intermediate valence region which

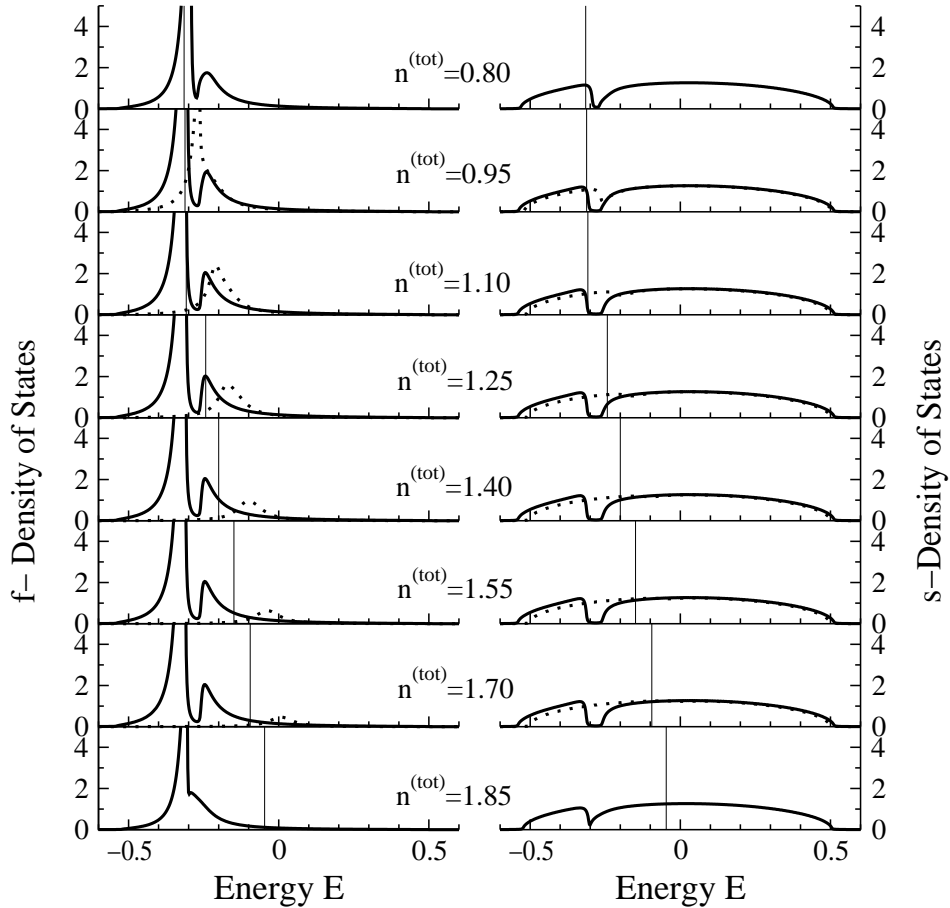


Figure 3. $f-$ and $s-$ quasiparticle densities of states for various values of $n^{(\text{tot})}$ and $e_f = -0.3$. Full lines for spin-up and dotted lines for spin-down. Other parameters are as in figure 1. Thin vertical lines show the position of chemical potential.

is investigated here. The quasiparticle density of states (Q-DOS), plotted in figure 3 for $e_f = -0.3\text{eV}$ and various electron densities, gives some evidence how to understand the sign change of the s -electron polarization. It is instructive to decompose the Q-DOS into s - and f -parts, although this decomposition is artificial because of the finite hybridization. The latter takes care for the fact that s - and f -partial-Q-DOS occupy exactly the same energy regions but of course with different weights. In the \uparrow -parts of both spectra the hybridization gap around $e_f = -0.3\text{eV}$ is clearly visible. For practically all densities $n^{(\text{tot})}$, exhibited in figure 3, the f -system is saturated, i. e. there are no down-spin f electrons. It is known from the Hubbard model [13, 15] and will be shown in figure 13 for the PAM, that then the damping of up-spin quasiparticles is in such a case negligible compared to that of down-spin quasiparticles. Fine structures like the hybridization gap are to be seen in the up-spectrum but not in the down-spectrum. The comparison with the SDA results in ref. [12] indeed confirms the interpretation that quasiparticle damping closes the hybridization gap in the \downarrow -spectrum. For the SDA neglects such damping effects, consequently the SDA- \downarrow -spectrum, too, exhibits a

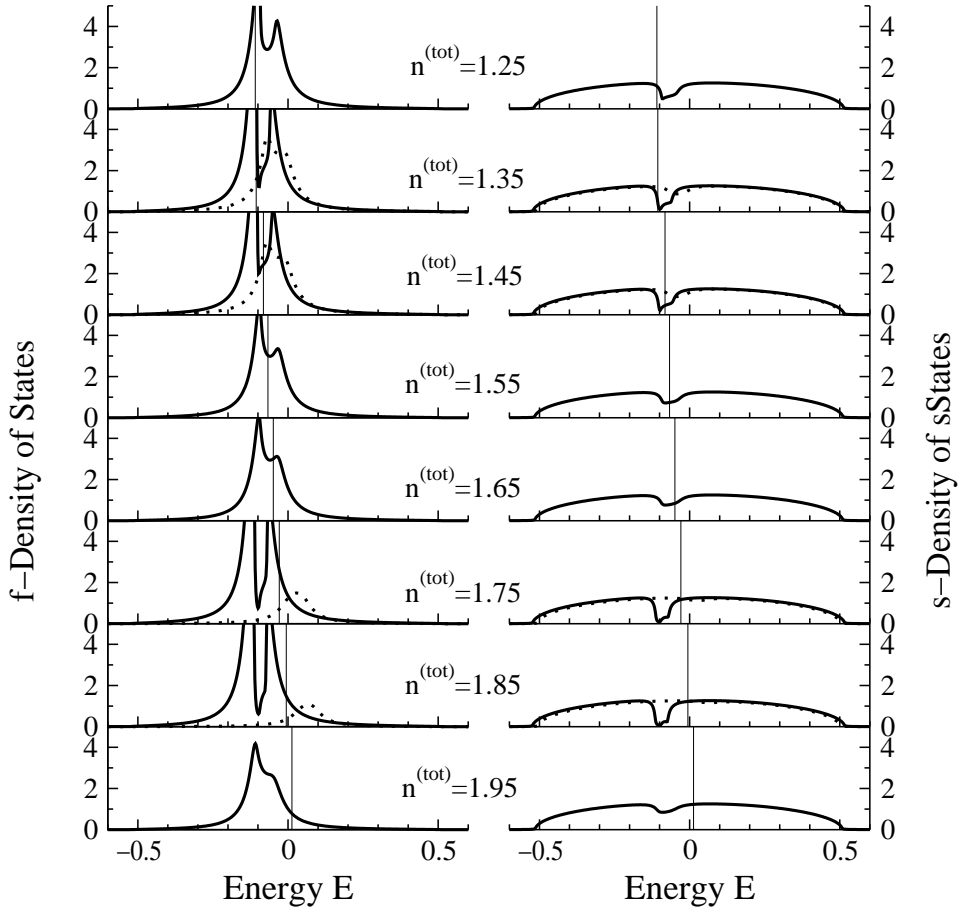


Figure 4. Same as figure 3 but $e_f = -0.1$.

gap. There is a slight exchange shift in the s -part due to hybridization. As long as the chemical potential μ is below the hybridization gap the system contains more up- than down-spin s -electrons, the s - f coupling is ferromagnetic. When μ shifts above the gap (in figure 3 in between $n^{(\text{tot})} = 1.10$ and $n^{(\text{tot})} = 1.25$), which exists only in the up-spectrum, then the increase in $n_{\downarrow}^{(s)}$ distinctly exceeds that of $n_{\uparrow}^{(s)}$, the s - f coupling becomes antiferromagnetic. That explains the magnetization behaviour in figure 2 (left column) as a density of states effect. Note, however, that the absolute value of the induced s -polarization is always rather small.

A qualitatively different situation is observed for the magnetization when e_f is near to the centre of the s -band (middle column in figure 2). A reentrant course appears, obviously not connected with the sign change of the s -polarization. It manifests itself in the phase diagram of figure 1 by the "oscillating" phase boundaries. Again a look at the respective Q-DOS is quite instructive. figure 4 shows the example $e_f = -0.1\text{eV}$. For such f -level position the hybridization gap splits the f -dominated part of the spectrum rather symmetrically into two almost equally weighted peaks. That holds in particular in the \uparrow -spectrum of the ferromagnetic phase ($n^{(\text{tot})} = 1.35, 1.45, 1.75, 1.85$ in figure 4). The chemical potential μ is located in one of the peaks, a situation which according to the

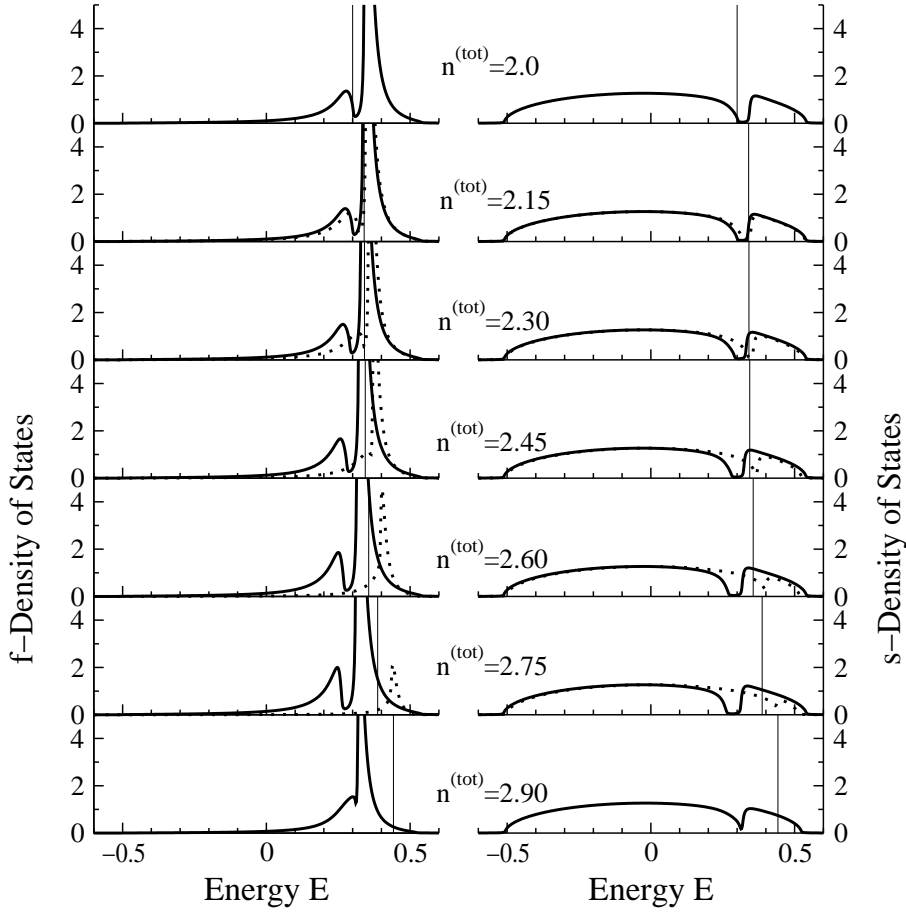


Figure 5. Same as figure 3 but $e_f = 0.3$.

simple Stoner criterion favours the appearance of ferromagnetism. As already discussed for the case of figure 3 (left column in figure 2) in the ordered phase \uparrow -quasiparticles are rather long-living while the \downarrow -particles are strongly damped. Again we conclude that this is the reason why the hybridization gap exists only in the \uparrow -spectrum. The spontaneous ferromagnetism disappears when μ enters the hybridization gap in accordance with the Stoner criterion. The quasiparticles are stronger damped in the paramagnetic phase than the \uparrow -particles in the ordered phase, so that the hybridization gap is more or less covered by the “smeared-out” quasiparticle peaks.

When the bare f -level e_f has been shifted into the upper half of the conduction band the polarization type changes once more. The coupling between s - and f -electrons is always antiferromagnetic (right column in figure 2). The Q-DOS in figure 5, concerning the case $e_f = 0.3\text{eV}$, reveals that ferromagnetic order sets in only when μ is above the hybridization gap. The consequence is that there are more s -electrons with spin \downarrow than spin \uparrow .

The phase diagram in figure 1 is calculated for a fixed hybridization $V = 0.1\text{eV}$. It is clear that V has a decisive influence on the extension of the ferromagnetic phase in the e_f - $n^{(\text{tot})}$ plane. Figure 6 demonstrates that the higher the hybridization V the

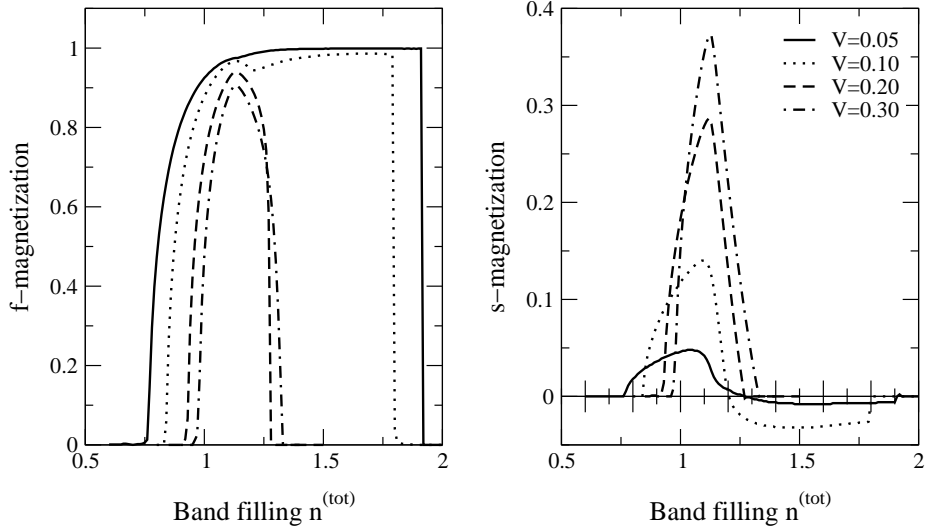


Figure 6. f - and s - magnetizations as a function of $n^{(\text{tot})}$ for different values of hybridization strength V with $e_f = -0.3$. Other parameters are as in figure 1.

smaller the ferromagnetic region. On the other hand, the induced polarization of the s -electrons increases with growing hybridization. Antiparallel coupling appears only for weak V . Strong electron fluctuations between s -band and f -level generally diminish magnetic stability but enhance the polarization of the s -band. However, the same hybridization is exclusively responsible for the ferromagnetic order. $V = 0$ does not permit ferromagnetism.

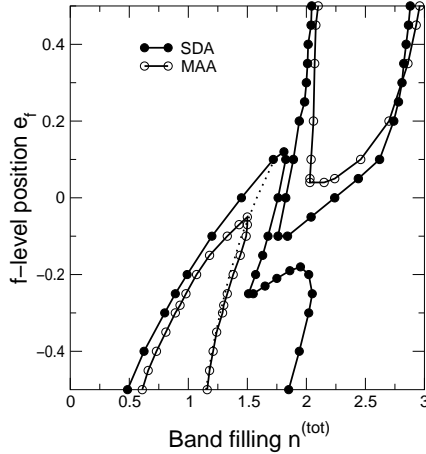


Figure 7. Magnetic phase diagram for MAA and SDA with $V = 0.2$, $U = 4$ and $T = 0$. f - and s - magnetizations are parallel to the left of the dotted line and anti-parallel to the right in the SDA. In the MAA f - and s - magnetizations are ant-parallel only when $n^{(\text{tot})} > 2$.

It is an interesting point to find out to what an extent quasiparticle damping may influence the possibility and the stability of ferromagnetic order. This can best be done by a comparison of the results found by SDA[12] and by MAA. Both methods are based

on the same physical ideas, MAA can be classified as "SDA plus quasiparticle damping". Figure 7 shows the magnetic phase diagram, derived within, respectively, SDA and MAA for the same set of model parameters. The e_f - $n^{(\text{tot})}$ area of the ferromagnetic phase is distinctly restricted in the MAA because of the quasiparticle damping, contrary to the SDA-result which is free of damping effects. For both methods we find that for lower particle densities a ferromagnetic, for higher densities an antiferromagnetic coupling of the s -electron spins to the local f -moments takes place.

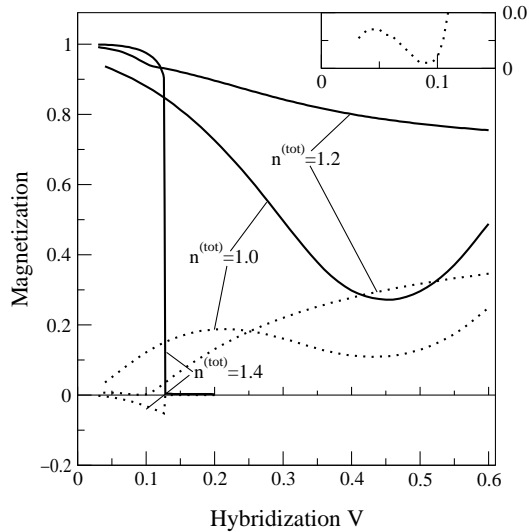


Figure 8. f - (solid line) and s - (dotted line) magnetizations as a function of hybridization strength V for different $n^{(\text{tot})}$ values for $e_f = -0.3$ at $T = 0$. The inset shows the s - magnetization for $n^{(\text{tot})} = 1.2$ in the region of small V .

Up to now we discussed mainly the e_f - and the $n^{(\text{tot})}$ -dependence of the physical properties of the periodic Anderson model. Let us now examine the influence of V in detail. Some results are plotted in figures 8, 9 and 10 for $e_f = -0.3\text{eV}$ and several particle densities $n^{(\text{tot})}$. The behaviour is not at all unique. For $n^{(\text{tot})} = 1.4$ a rather weak hybridization V is sufficient to destroy the ferromagnetism (figure 8). The Curie temperature T_c runs through a maximum (figure 9) pointing therewith to the fact that V provokes two competing effects. It broadens the f -level, thus creating the precondition for a magnetic order (no ferromagnetism in the zero-bandwidth Hubbard model [30]!). On the other hand, increasing s - f fluctuations must damage the ferromagnetic order because the empty f -level does not carry a magnetic moment. It is remarkable that T_c goes smoothly to zero (figure 9) although the $T = 0$ -magnetization performs a first-order transition (figure 8).

A completely different V -dependence shows up for the band occupations $n^{(\text{tot})} = 1.0$ and 1.2. In these cases large hybridization strength does not destroy the ferromagnetism, but rather enhances T_c . By closely examining figure 8, one recognizes a "kink" or a minimum in the respective magnetization curves, for $n^{(\text{tot})} = 1.0$ at $V \approx 0.45$ and for $n^{(\text{tot})} = 1.2$ at $V \approx 0.09$. By comparing with the densities of states (figure 10),

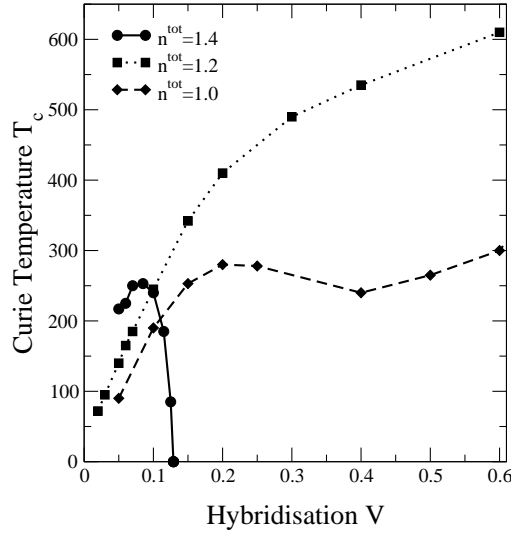


Figure 9. Curie Temperature T_c as a function of V for different values of $n^{(\text{tot})}$ with $e_f = -0.3$.

we note that this value approximately coincides with the V -value where μ enters the hybridization gap in the \uparrow -Q-DOS. I. e. the system becomes a semimetal where only the \downarrow -electrons contribute to the electrical current. One might speculate that this has something to do with the increasing T_c . However, we cannot rule out the possibility that this is an effect of our approximation rather than an inherent property of the PAM.

Let us finally discuss the temperature-dependence of the magnetic properties as, e. g., the spontaneous magnetization (figure 11). First order as well as second order transitions appear. Whether first order transitions are artefacts of our approximate procedure or intrinsic properties of the PAM is not clear. A similar situation is found when applying the MAA to the Hubbard model [24]. In case of a second-order transition the f -magnetization behaves like a Brillouin function, while the corresponding induced s -polarization very often shows remarkable deviations. The examples plotted in figure 11 demonstrate again that the s - f coupling may be ferromagnetic or antiferromagnetic depending on the band filling.

A key-quantity of ferromagnetism is the Curie-temperature T_c , which is of course decisively influenced by the bandfilling (figure 12). The $n^{(\text{tot})}$ -dependence is very much more regular than the V -dependence exhibited in figure 9. The reentrant behaviour for $e_f = -0.1\text{eV}$ corresponds to that of the $T = 0$ -moment in figure 2 (middle column). The calculated T_c -values are of a realistic order of magnitude. The transition into the paramagnetic phase ($T_c = 0$) seems to be always continuous even if the break-down of the $T = 0$ -moment is discontinuous (figure 2). The temperature-dependence of the magnetization is due to a respective behaviour of the Q-DOS (figure 13). There is a distinct spin asymmetry in the lower f -like peak ("lower Hubbard band") which causes the spontaneous magnetic moment. The up-spin part is characterized by a hybridization gap, which is not visible in the down-spin spectrum (cf. figures 3, 4 and 5). As already

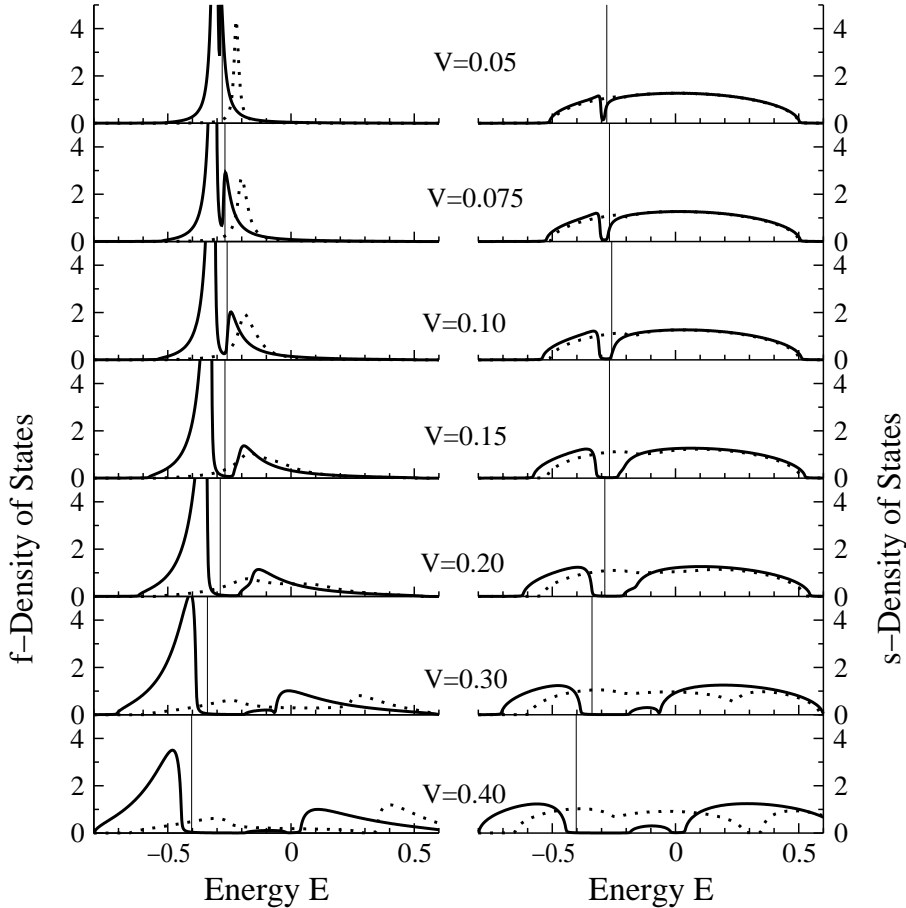


Figure 10. f - and s - quasiparticle densities of states for various values of V with $e_f = -0.3$ and $n^{(\text{tot})} = 1.2$ at $T = 0$. Full lines for spin-up and dotted lines for spin-down. Thin vertical lines show the position of chemical potential.

mentioned, this is due to quasiparticle damping, which for low temperatures is very much stronger for \downarrow - than for \uparrow -quasiparticles (cf. figure 13). With increasing temperature the damping of the \uparrow -particles, is getting larger and that of the \downarrow particles smaller. For increasing temperatures, a dip develops in the spin- \downarrow Q-DOS, which eventually merges with the spin- \uparrow hybridization gap at $T = T_c$. The spin asymmetry is then removed. The induced spin polarization of the conduction band is always very weak so that the assumption that the collective order is based on an RKKY-like coupling via the polarized conduction electrons appears unlikely. It is rather to believe that the observed ferromagnetism is due to strong electron correlations in the narrow "f-band" as it happens in the single-band Hubbard model [25, 33]. The coupling to the s -band via V takes care for the finite width of the original f -level being in this sense the basic precondition for ferromagnetic order in the periodic Anderson model.

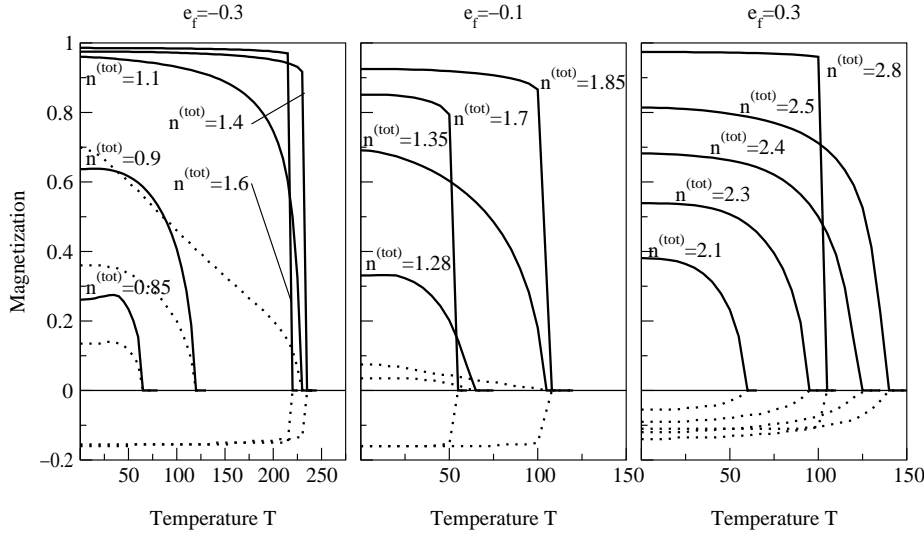


Figure 11. f - (solid line) and s - (dotted line) magnetization as a function of temperature for various e_f and $n^{(\text{tot})}$ as mentioned in the figure. s - magnetization is multiplied by a factor of 5 for better clarity.

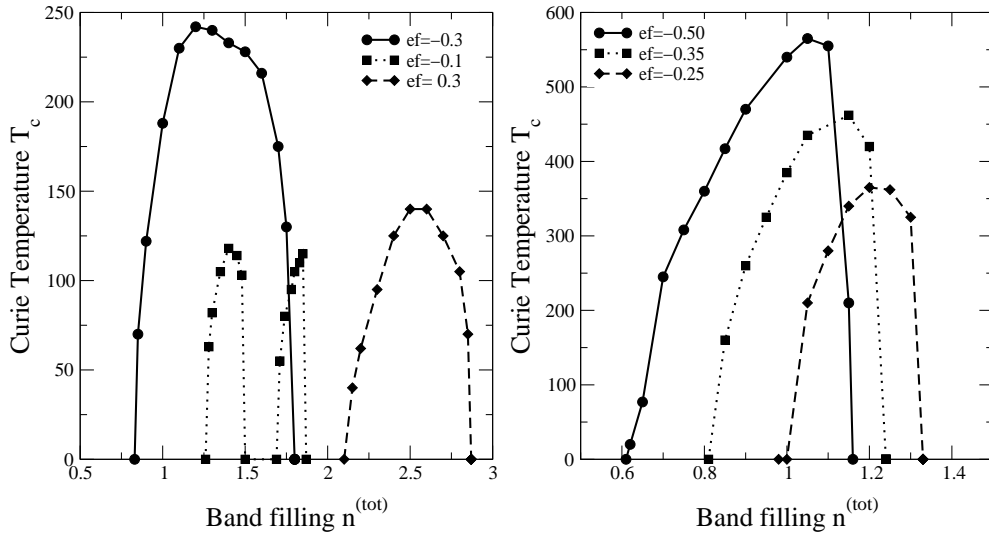


Figure 12. Curie temperature T_c as a function of band filling $n^{(\text{tot})}$ for different values of e_f . The hybridization strength $V = 0.1$ for the left and $V = 0.2$ for the right of figure.

5. Conclusion

A "modified alloy analogy" (MAA) [25, 24], previously introduced as an approach to the single-band Hubbard model [30] has been applied to the periodic Anderson model (PAM). A high-energy expansion of relevant Green functions as well as a corresponding expansion of the determination equation for the CPA-self-energy have been used to find the optimum alloy analogy for the PAM. This alloy analogy is then used to solve the PAM-many body problem within the CPA. By construction the MAA represents

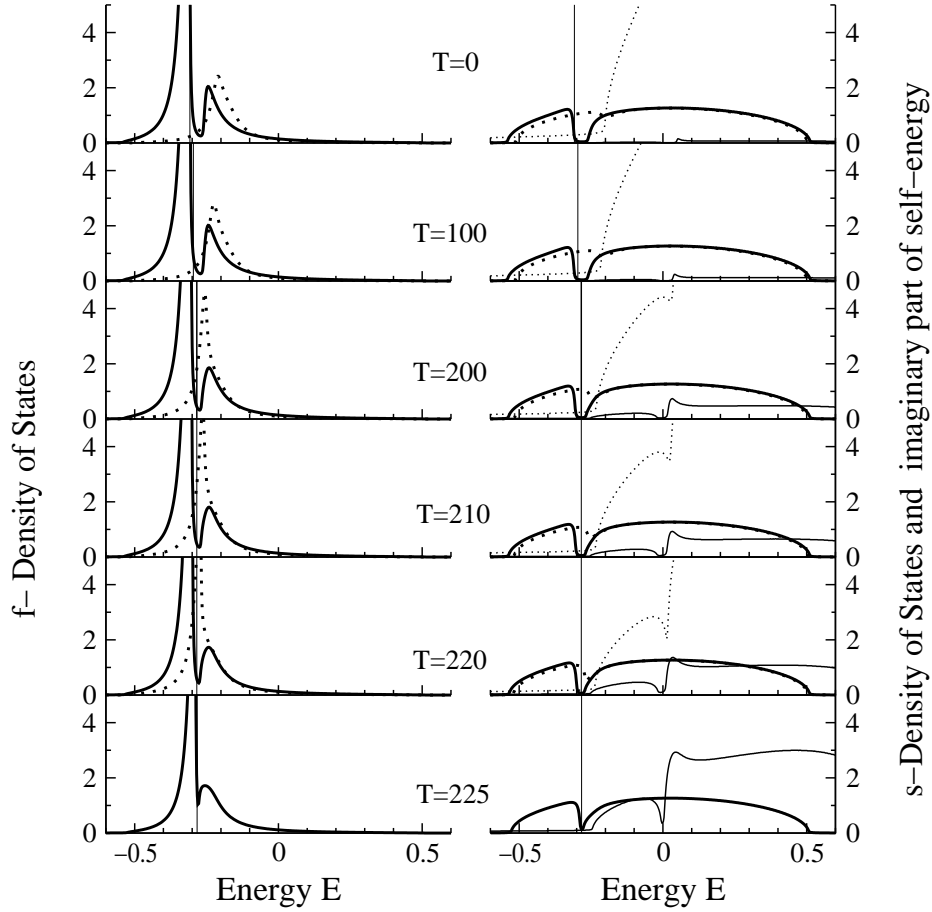


Figure 13. f - and s - quasiparticle densities of states at various temperatures. $e_f = 0.3$, $V = 0.1$ and $n^{(\text{tot})} = 1.1$. Full lines for spin-up and dotted lines for spin-down. Thin vertical lines show the position of chemical potential. Additionally, the imaginary part of the self-energy is plotted as thin lines in the right column. For better visibility, it is multiplied by -100 .

a strong-coupling approach, therewith most probably suitable to describe spontaneous ferromagnetism in the PAM. It can be considered as an extension and improvement of the "spectral density approach" (SDA) [13, 14, 15, 24], mainly by inclusion of quasiparticle damping. It cannot reproduce, however, the low-energy features of the PAM (Kondo resonance)[1, 34], being certainly not so decisive with respect to magnetic stability. It incorporates, however, important higher correlation functions ("spin-dependent band shift") which guarantee the correct strong-coupling behaviour [21].

The present study focuses on the possibility and the stability of ferromagnetism in the PAM: Magnetic phase diagrams are constructed in terms of relevant model parameters such as hybridization strength V , f -level position e_f and total particle density $n^{(\text{tot})}$. For this work we are mainly interested in the intermediate valence regime, i. e. that e_f is chosen within the energy region of the "free" Bloch band. The same holds for the chemical potential μ . As usual "f-level" and conduction band, respectively, are assumed as non-degenerate. The intraatomic Coulomb interaction U of the f electrons

leads to a splitting of e_f into two sublevels at e_f and $e_f + U$. U is chosen so that the upper charge excitation remains unoccupied i. e. $0 < n^{(\text{tot})} < 3$. The influence of V is multifold. First of all it provokes a finite width of the lower f -quasiparticle peak that turns out a basic prerequisite for ferromagnetism in the intermediate valence PAM. On the other hand, too strong s - f fluctuations due to V destabilize the ferromagnetic order. Additionally V provokes a hybridization gap in the energy spectrum, which, however, is getting closed by too strong quasiparticle damping. If the f -magnetization is almost saturated then the \uparrow -spectrum shows a hybridization gap, the \downarrow -spectrum not. This has some influence on the induced s -polarization which can be parallel or antiparallel to the f -moment. The derived Curie temperatures are of reasonable orders of magnitude. All magnetic properties of PAM can be illustratively traced back and reasoned by inspection of the respective quasiparticle density of states.

References

- [1] A. C. Hewson, *The Kondo Problem to Heavy Fermions*, Cambridge University Press 1993.
- [2] A. M. Tsvelick and P. B. Wiegmann, Adv. Phys. **32**(4), 453 1983.
- [3] K. Wilson, Rev. Mod. Phys. **47**(4), 773 1975.
- [4] W. Metzner and D. Vollhardt, Phys. Rev. Lett. **62**, 324 1989.
- [5] T. Pruschke, M. Jarrell, and J. K. Freericks, Adv. Phys. **44**(2), 187 1995.
- [6] A. Georges, G. Kotliar, W. Krauth, and M. J. Rozenberg, Rev. Mod. Phys. **68**(1), 13 1996.
- [7] R. Bulla, A. C. Hewson, and T. Pruschke, J. Phys.: Condens. Matter **10**, 8365 1998.
- [8] D. Meyer, T. Wegner, M. Potthoff, and W. Nolting, Physica B **270**, 225 1999.
- [9] J. R. Schrieffer and P. A. Wolff, Phys. Rev. **149**(2), 491 1966.
- [10] S. Doniach, Physica B **91**, 231 1977.
- [11] A. P. Ramirez, J. Phys.: Condens. Matter **9**, 8171 1997.
- [12] D. Meyer, W. Nolting, G.G. Reddy, and A. Ramakanth, phys. stat. sol. (b) **208**, 473 1998.
- [13] G. Geipel and W. Nolting, Phys. Rev. B **38**, 2608 1988.
- [14] W. Nolting and W. Borgiel, Phys. Rev. B **39**(10), 6962 1989.
- [15] T. Herrmann and W. Nolting, J. Magn. Magn. Mat. **170**, 253 1997.
- [16] B. Velicky, S. Kirkpatrick, and H. Ehrenreich, Phys. Rev. **175**, 747 1968.
- [17] J. Hubbard, Proc. R. Soc. London, Ser. A **281**, 401 1964.
- [18] H. J. Leder and G. Czycholl, Z. Phys. B **35**, 7 1979.
- [19] G. Czycholl, Physics Reports **143**(5), 277 1986.
- [20] R. Vlammung and D. Vollhardt, Phys. Rev. B **45**, 4637 1992.
- [21] A. Harris and R. Lange, Phys. Rev. **157**(2), 295 1967.
- [22] G. Bulk and R. J. Jelitto, Phys. Rev. B **41**, 413 1990.
- [23] M. Potthoff and W. Nolting, Z. Phys. B **104**, 265 1997.
- [24] M. Potthoff, T. Herrmann, T. Wegner, and W. Nolting, phys. stat. sol. (b) **210**, 199 1998.
- [25] T. Herrmann and W. Nolting, Phys. Rev. B **53**(16), 10579 1996.
- [26] H. Fukuyama and H. Ehrenreich, Phys. Rev. B **7**, 3266 1973.
- [27] J. Schneider and V. Drehel, phys. stat. sol. (b) **68**, 207 1975.
- [28] D. Meyer and W. Nolting, Physica B **281**, 189 2000.
- [29] T. Herrmann and W. Nolting, Phys. Rev. B **60**, 12861 1999.
- [30] J. Hubbard, Proc. R. Soc. London, Ser. A **276**, 238 1963.
- [31] J. Wahle et al, Phys. Rev. B **58**, 12749 1998.
- [32] P. W. Anderson, In F. Seitz and D. Turnbull, editors, *Solid State Physics: Advances in Research and Applications* volume 14 page 99. Academic Press New York 1963.

- [33] T. Herrmann and W. Nolting, Solid State Commun. **103**(6), 351 1997.
- [34] M. Jarrell, Phys. Rev. B **51**(12), 7429 1995.

Acknowledgments

We wish to thank T. Herrmann for very helpful discussions. Financial support by the *Volkswagen-Foundation* within the project “*Phasendiagramm des Kondo-Gitter-Modells*” is gratefully acknowledged. One of us (D. M.) wants to thank the *Friedrich-Naumann-Foundation* for supporting his work.